

HIGH-VELOCITY IMPACT EXPERIMENTS OF SIMULATED POROUS ASTEROIDS AND MEASUREMENTS OF POST IMPACT TEMPERATURE AROUND IMPACT CRATER. M. Yasui¹, T. Tazawa¹, R. Hashimoto¹, M. Arakawa¹, and K. Ogawa², ¹Graduate School of Science, Kobe University, Japan (minami.yasui@pearl.kobe-u.ac.jp), ²JAXA Space Exploration Center.

Introduction: A heat source triggers aqueous alteration and creation of organic solid materials in the parent bodies of asteroids. For example, the mineralogical analysis of carbonaceous chondrites delivered from C-type asteroids showed that their parent bodies had been experienced heating up to 50–150 °C [1, 2]. Radioactive heating of ²⁶Al, is one of the plausible heat sources but this efficiency might depend on the timing of the accretion of the parent bodies.

Another plausible heat source is impact-generated heating. The collision among parent bodies of asteroids at the relative velocity of 4–5 km/s[3] would have induce high shock pressure and the associated shock heat would have raised the temperature around the impact crater instantaneously. These collisions are a common phenomenon and this shock heat would have effectively worked for porous bodies such as asteroids having low bulk density because the attenuation rate of the shock pressure is very large. However, the effects of impact heating have not been directly studied in the laboratory experiments.

In this study, we performed high-velocity impact cratering experiments on simulated parent bodies of asteroids in order to study the effects of impact heating on the cratering processes. So, we tried to measure the temperature around the impact crater directly and investigated the heat generation and dissipation during the impacts [4].

Experimental Method: We used a porous gypsum block with a porosity of 50% as a target simulating porous asteroids. In order to measure the temperature directly during the impact, 4–5 chromel-alumel thermocouples were set in the target at a constant depth from the target surface, and at different distances from the impact point, L : The L was changed from 17.8 to 8.5 mm. The measured temperatures were recorded by a data logger with an A/D conversion rate of 10 kHz.

Impact experiments were performed by using a two-stage gas gun at Kobe University. We used two kinds of spherical projectiles, a 4.75-mm diameter polycarbonate and a 2-mm diameter aluminum. The impact velocity ranged from 5.0 to 1.1 km/s. The target chamber was evacuated below 25 Pa before each shot. The ambient temperature in the target chamber was ~20 °C. In order to observe the impact phenomena by a high-speed camera, we used two metal halide lamps but they were turned on and off just before and after the impact to prevent the temperature rise.

Results: Temperature change. Fig. 1 shows examples of the temperature change with time at different values of L . The temperature change, ΔT , on the vertical axis means the temperature difference between before and after the impact. At small L , the ΔT rose drastically just after the impact and then it dropped gradually as the time passed. On the other hand, the ΔT rose gradually and it dropped more gradually as the L was larger. Moreover, the maximum ΔT decreased with increasing the L . This trend was also confirmed on the results for other impact velocities and projectile types.

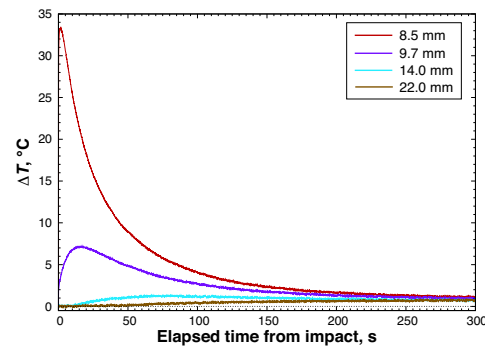


Fig. 1: Temperature change with time for a polycarbonate projectile impacted at 1.7 km/s at the L of 8.5–22.0 mm.

In this study, we analyzed the maximum temperature, ΔT_{\max} , and the half width of the temperature peak, Δt_{half} . Then, we examined the relationship between these parameters and the L .

Maximum temperature. Fig. 2 shows the relationship between the ΔT_{\max} and the L normalized by the crater radius R . The ΔT_{\max} decreased exponentially with increasing the normalized distance, L/R . Moreover, most of the data merged well, irrespective of projectile type and impact velocity. The relationship is approximated by one power law equation, $\Delta T_{\max} = 288.4(L/R)^{-4.02}$.

Next, we calculated the temperature change by using one-dimensional heat conduction model, and then the result of numerical simulations were compared with our experimental results. In this calculation, the temperature around the impact crater was assumed to be controlled by only heat conduction of the post-shock heat deposited on the crater floor just after the impact. So, a shell with a thickness, n , on the crater floor was heated at an initial temperature, T_i , by the post-shock heat, and

the heat was diffused by only thermal conduction to the interior of the target from the crater floor. The calculation result is also shown in Fig. 2 (dotted line). The T_i and n , by which the experimental results could be reproduced well, were obtained to be 110 °C and 3 mm; 110 °C corresponds to the temperature on the crater floor just after the impact measured by IR camera, and 3 mm was comparable with the projectile diameter.

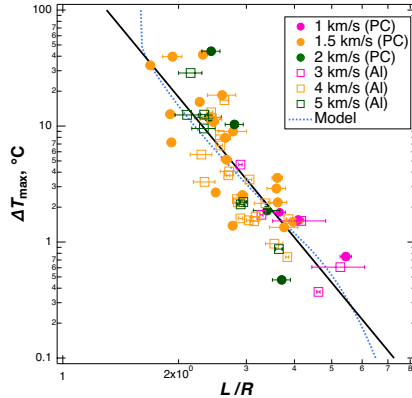


Fig. 2: Maximum temperature, ΔT_{\max} , vs. normalized distance, L/R . The black solid line represents the fitting line, and the blue dotted line represents the numerical results.

Heating Duration: Fig. 3 shows the relationship between the Δt_{half} normalized by the thermal diffusion time, τ , and the normalized distance, L/R . The τ is defined by $k/\rho_t c$, where k is the thermal conductivity (0.42 W/m·K, measured in this study), ρ_t is the target density (1030 kg/m³), c is the specific heat (1050 J/kg·K). The normalized Δt_{half} was well scaled and it increased with increasing the L/R , irrespective of projectile type and impact velocity. The relationship is approximated by one quadratic function when the $\Delta t_{\text{half}}/\tau = 0$ at $L/R = 1$, $\Delta t_{\text{half}}/\tau = -0.257 + 0.004(L/R) + 0.253(L/R)^2$.

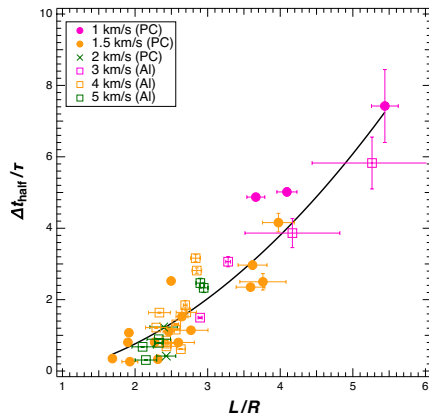


Fig. 3: Half width, Δt_{half} , vs. normalized distance, L/R . The black solid line represents the fitting line.

Discussion: Finally, we discussed the possibility of occurrence of aqueous alteration and organic solid formation below the crater floor by impact heating on the parent bodies of asteroids. Here, we used our empirical equations of ΔT_{\max} and Δt_{half} and set the critical temperature necessary for the above processes as 50–150 °C [2] for aqueous alteration and 0–100 °C [5] for organic solid formation. Their durations was reported to be 4 Ma for aqueous alteration [6] and several tens of days to kyr depending on the temperature for organic solid formation [7]. As a result, impacts producing the craters with the radius larger than 20 km and 1 km could facilitate aqueous alteration and organic solid formation at 0 °C, respectively, at distances within 2 AU. Moreover, at distances within 4 AU, the temperature just below the crater floor of craters with the radius of 100 m could rise up to 100 °C, so organic solid formation could also facilitate.

References: [1] McSween H. Y. Jr. (1987) *Geochim. Cosmochim. Acta*, 51, 2469–2477. [2] Zolensky M. E. et al. (1989) *Icarus*, 78, 411–425. [3] Bottke W. F. Jr. et al. (1994) *Icarus*, 107, 255–268. [4] Yasui, M. et al. (2021) *Comm. Earth & Environ.*, 2, 95. [5] Kebukawa, Y. & Cody, G. D. (2015) *Icarus*, 248, 412–423. [6] de Leuw, S. et al. (2009) *Geochim. Cosmochim. Acta*, 73, 7433–7442. [7] Briani, G. et al. (2013) *Geochim. Cosmochim. Acta*, 122, 267–279.